

Niobium doped TiO₂ : Intrinsic transparent metallic anatase versus highly resistive rutile phase

S. X. Zhang, D. C. Kundaliya, W. Yu, S. Dhar, S. Y. Young, L. G. Salamanca-Riba, S. B. Ogale, R. D. Vispute, and T. Venkatesan

Citation: *Journal of Applied Physics* **102**, 013701 (2007); doi: 10.1063/1.2750407

View online: <http://dx.doi.org/10.1063/1.2750407>

View Table of Contents: <http://scitation.aip.org/content/aip/journal/jap/102/1?ver=pdfcov>

Published by the [AIP Publishing](#)

Articles you may be interested in

[Low temperature resistivity, thermoelectricity, and power factor of Nb doped anatase TiO₂](#)

Appl. Phys. Lett. **102**, 013901 (2013); 10.1063/1.4773517

[Transparent semiconducting Nb-doped anatase TiO₂ films deposited by helicon-wave-excited-plasma sputtering](#)

J. Vac. Sci. Technol. B **29**, 011017 (2011); 10.1116/1.3525918

[Growth parameter-property phase diagram for pulsed laser deposited transparent oxide conductor anatase Nb : Ti O₂](#)

Appl. Phys. Lett. **91**, 112113 (2007); 10.1063/1.2785152

[Response to "Comment on 'A transparent metal: Nb-doped anatase Ti O₂ ' \[Appl. Phys. Lett.86, 252101 \(2005\)\]"](#)

Appl. Phys. Lett. **88**, 226103 (2006); 10.1063/1.2208448

[A transparent metal: Nb-doped anatase Ti O₂](#)

Appl. Phys. Lett. **86**, 252101 (2005); 10.1063/1.1949728



Re-register for Table of Content Alerts

Create a profile.



Sign up today!



Niobium doped TiO₂: Intrinsic transparent metallic anatase versus highly resistive rutile phase

S. X. Zhang,^{a)} D. C. Kundaliya, W. Yu, and S. Dhar

Center for Superconductivity Research, Department of Physics, University of Maryland, College Park, Maryland 20742

S. Y. Young and L. G. Salamanca-Riba

Department of Materials Science and Engineering, University of Maryland, College Park, Maryland 20742

S. B. Ogale,^{b)} R. D. Vispute, and T. Venkatesan

Center for Superconductivity Research, Department of Physics, University of Maryland, College Park, Maryland 20742-4111

(Received 3 April 2007; accepted 9 May 2007; published online 2 July 2007)

We report on the structural, electrical, and optical properties of 5% niobium doped TiO₂ thin films grown on various substrates by pulsed laser deposition. The epitaxial anatase Nb:TiO₂ film on LaAlO₃ is shown to be an intrinsic transparent metal and its metallic property arises from Nb substitution into Ti site as evidenced by the Rutherford backscattering channeling result. In contrast, the rutile Nb:TiO₂ thin films show insulating behaviors with 2–3 orders higher room temperature electrical resistivity and ~ 30 times lower mobility. A blueshift in the optical absorption edge is observed in both phases, though of differing magnitude. © 2007 American Institute of Physics. [DOI: 10.1063/1.2750407]

I. INTRODUCTION

In the field of electronics, considerable efforts have been dedicated to the study of transparent conducting oxides (TCO) due to the expanding demand for transparent electrodes in optoelectronic devices such as flat panel displays (FPDs), organic light emitting displays (OLEDs), etc.^{1–3} Currently tin-doped indium oxide (ITO), with excellent conductivity ($\rho_{RT} \sim 10^{-4}$ Ω cm) and high transmittance ($\sim 90\%$) in the visible range, is in practical use for most transparent electrode applications. However, due to the cost and scarcity of indium, ITO may not be able to satisfy the demands in the future and, hence, the search for new TCO has become very significant.

TiO₂ has three different structural polymorphs: rutile, anatase, and brookite. The rutile phase, the most stable one, has been extensively studied^{4–6} over decades because of its potential technological importance in catalysis,⁷ electrochromism,⁸ and photocatalysis.⁹ In contrast, much less experimental work is reported on the anatase phase partly due to the difficulty in synthesizing good-quality single crystals.^{10,11} The few reported studies have shown significant differences between the electrical, magnetic, and optical properties of the anatase and rutile phases.^{12–14} Recently, the observation of high temperature ferromagnetism with some magnetic dopants into anatase TiO₂ has triggered great interest in this material in the field of spintronics.^{15,16} However, there are hardly any detailed reports on the electrical properties of anatase TiO₂ doped by transition elements or other multivalent elements from a pure semiconductor technology point of view. Most recently, Furubayashi *et al.*¹⁷ reported

the discovery of Nb-doped anatase TiO₂ as a new TCO. It was shown that the room temperature (RT) resistivity of this material with Nb concentration $>3\%$ grown on a SrTiO₃ (001) single crystal is $2\text{--}3 \times 10^{-4}$ Ω cm and the transmittance in the visible range is $\sim 90\%$. However, the origin and the precise nature of transparent metallic properties of Nb:TiO₂ invites further scrutiny because of the possibility of niobium diffusion into SrTiO₃ forming Nb:SrTiO₃, which also shows good conductivity at certain growth conditions.^{18,19} Toward this end we have performed a systematic study of the structural, electrical, and optical properties of 5% Nb:TiO₂ (NTO) films grown on various substrates. Our results show that Nb-doped TiO₂ with a single crystalline anatase phase is indeed an intrinsic TCO and its metallic property arises from Nb substitution into the Ti site which provides electrons into the conduction band. However, its rutile phase shows insulating behavior with 2–3 orders higher room temperature resistivity. Possible reasons for these differences are addressed.

II. EXPERIMENT

The 5% Nb:TiO₂ thin films with a thickness of ~ 800 Å were grown on single crystal (001) LaAlO₃ (LAO), SrTiO₃ (STO), *r*-(*c*)-plane sapphire and quartz substrates, at the same growth conditions as reported by Furubayashi *et al.*¹⁷ via pulsed laser deposition. X-ray diffraction patterns (as shown in Fig. 1) indicate that the films grown on (001) LAO and STO substrates were epitaxial with single phase anatase character and (00*L*) orientation. However, the films grown on *r*- and *c*-sapphire substrates are epitaxial and of rutile phase with the (101) and (*L*00) orientations, respectively. The NTO film on quartz (SiO₂) forms the polycrystalline rutile phase.

^{a)}Electronic mail: sxzhang@umd.edu

^{b)}Present address: National Chemical Laboratory, Pune, India; electronic mail: sb.ogale@ncl.res.in

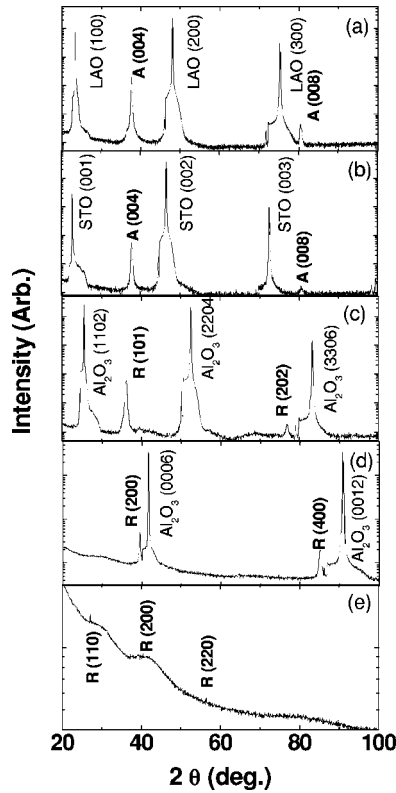


FIG. 1. X-ray diffraction patterns for (a) NTO/LAO, (b) NTO/STO, (c) NTO/*r*-Al₂O₃, (d) NTO/*c*-Al₂O₃, and (e) NTO/quartz thin films.

III. RESULTS AND DISCUSSION

Figures 2(a) and 2(b) show the Rutherford backscattering spectra (random and channeled) for 5% Nb:TiO₂ (NTO) films grown on (001) LAO and STO, respectively. The minimum channeling yield of Ti and Nb in NTO/LAO are both $\sim 10\%$, indicating that about 90% Nb substitutes into the Ti site, while those for NTO/STO are about 50%, suggesting that NTO/LAO has a much better crystalline quality than NTO/STO. The better crystalline quality of NTO/LAO could

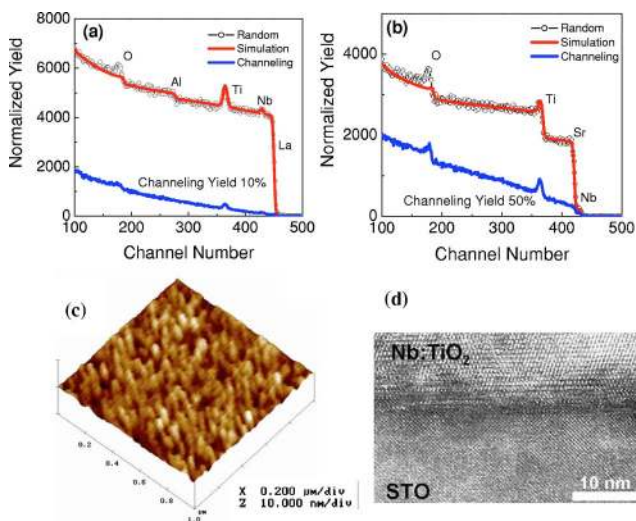


FIG. 2. (Color online) Rutherford backscattering-ion channeling spectrum obtaining from (a) NTO/LAO and (b) NTO/STO films and (c) AFM image of NTO/LAO film. (d) High-resolution TEM image at the interface of Nb:TiO₂ film and SrTiO₃ substrate.

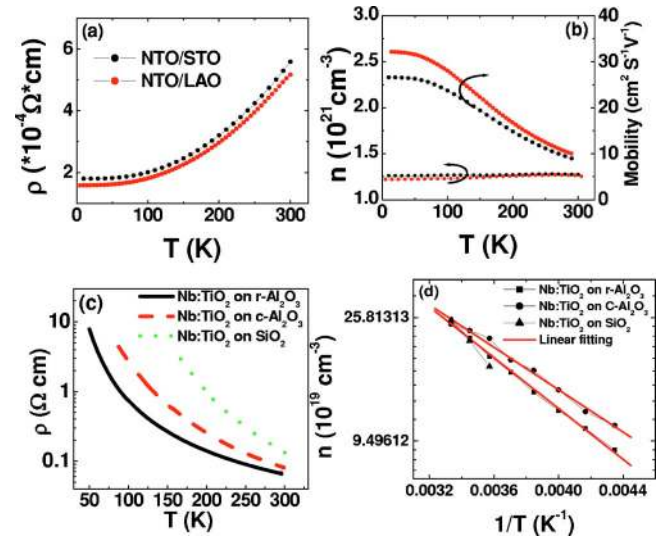


FIG. 3. (Color online) Temperature dependence of (a) resistivity and (b) carrier density and Hall mobility for NTO/STO (black curves) and NTO/LAO (red curves); (c) temperature dependence of resistivity for NTO/*r*-Al₂O₃ (black solid line), NTO/*c*-Al₂O₃ (red dashed line), and NTO/quartz (green dotted line). (d) Carrier density as a function of $1/T$ for NTO/*r*-Al₂O₃ (square dots), NTO/*c*-Al₂O₃ (round dots), and NTO/quartz (up triangle dots), red curves are fitting data.

be attributed to the lower lattice mismatch between TiO₂ and LAO ($\sim -0.26\%$) than that between TiO₂ and STO ($\sim -3.1\%$). This argument is further evidenced by the x-ray diffraction rocking curves (full width at half maximum of the anatase (004) peak are 0.42° and 0.93° for NTO/LAO and NTO/STO, respectively) and the atomic force microscopy (AFM) measurements. Figure 2(c) shows the AFM image of the surface of NTO/LAO, which is very smooth (mean roughness ~ 0.344 nm). While the film on STO (not shown) is much rougher, with a mean roughness of ~ 1.050 nm.

We investigate the interface nanostructure of NTO/STO by using high-resolution transmission electron microscopy (TEM). As shown in the Fig. 2(d) TEM cross-section image, the film is epitaxially grown as an anatase phase. The slightly distorted NTO nanostructure along the interface is caused by the misfit dislocations, stress at early stage deposition, and 2–3 atomic-level steps on the original STO substrate surface. We were unable to conclude whether there is any interdiffusion of niobium in STO and contributing to the excellent conductivity of the NTO/STO sample. Since no extrinsic conducting layer forms when Nb diffuses into LAO and moreover our cobalt doped NTO/LAO has been shown not to exhibit interdiffusion even when grown at very high temperature (850°C),²⁰ in the following we mainly focus on the properties of the films grown on (001) LAO substrate when we discuss the properties of anatase Nb:TiO₂.

Figure 3(a) compares the temperature dependence of resistivity for NTO/LAO and NTO/STO. Both samples show metallic behavior with the RT resistivity of $4.95 \times 10^{-4} \Omega \text{ cm}$ for the NTO/LAO and $5.59 \times 10^{-4} \Omega \text{ cm}$ for the NTO/STO (calculation based on the assumption that no interface Nb:SrTiO₃ contribution is present). These results confirm the report by Furubayashi *et al.*^{17,19} As shown in Fig. 3(b), the carrier densities in the film on LAO are $\sim 1.25 \times 10^{21} \text{ cm}^{-3}$ at room temperature and almost independent of

TABLE I. The comparison of room temperature resistivities, carrier densities, and Hall mobilities of NTO thin films grown at various substrates.

Samples	RT resistivity ρ_{RT} (Ω cm)	RT carrier density n_{RT} (cm^{-3})	RT Hall mobility μ_{RT} ($\text{cm}^2 \text{V}^{-1} \text{S}^{-1}$)
Anatase 5% Nb:TiO ₂ on LAO	4.95×10^{-4}	1.25×10^{21}	10
Anatase 5% Nb:TiO ₂ on STO	5.59×10^{-4}	1.26×10^{21}	8.9
Rutile 5% Nb:TiO ₂ on <i>r</i> -Al ₂ O ₃	0.066	2.55×10^{20}	0.379
Rutile 5% Nb:TiO ₂ on <i>c</i> -Al ₂ O ₃	0.08	2.42×10^{20}	0.323
Rutile 5% Nb:TiO ₂ on quartz	0.13	2.40×10^{20}	0.199

temperature. We can get the carrier density versus Nb concentration $\sim 90\%$, which is identical to the Nb substitution rate ($\sim 90\%$) in NTO/LAO obtained from channeling. Figure 3(b) also shows the Hall mobilities μ_H , which increase from 10 to 33 $\text{cm}^2 \text{V}^{-1} \text{S}^{-1}$ as temperature decreases from RT to 10 K. We also show the temperature dependence of the carrier density and Hall mobility data of our NTO/STO sample in Fig. 3(b) (again on the assumption that no contribution emanates from the interface Nb:SrTiO₃ layer) just for comparison with the NTO/STO data reported by Furubayashi *et al.*,¹⁷ which show similar behavior.

Figure 3(c) shows the electrical properties of three rutile Nb:TiO₂ thin films grown on *r*-sapphire, *c*-sapphire, and quartz substrates. All the resistivity versus temperature ($R-T$) curves show negative slope indicating semiconducting (or insulating) properties. Figure 3(d) shows the carrier density n as a function of $1/T$ for these three samples (Hall measurements could only be performed above 230 K due to the high resistance at low temperatures, carrier density was obtained by simply assuming Hall mobility is almost equal to drift mobility). In contrast to the case of anatase, carrier density decreases quickly as temperature decreases and $\ln(n)$ is almost linear to $1/T$. By fitting the data, we can get the electron activation energy ε of ~ 0.075 and ~ 0.088 eV for NTO/*c*- and NTO/*r*-sapphire, respectively. This indicates that rutile NTO is a thermal activated semiconductor, while anatase NTO is a degenerate semiconductor. In Table I, we compared the room temperature resistivity, carrier density, and Hall mobility of all the samples. The room temperature resistivities are found to be 0.066 Ω cm for NTO/*r*-Al₂O₃, 0.08 Ω cm for NTO/*c*-Al₂O₃, and 0.13 Ω cm for NTO/SiO₂, all of which are 2–3 orders higher than the values for epitaxial anatase films grown on (001) LAO. These results are consistent with the report by Furubayashi *et al.*¹⁹ However, it is found that the RT carrier densities ($\sim 2.4 \times 10^{20} \text{ cm}^{-3}$) of these three rutile films are only five times lower than that of the single crystalline anatase phase, suggesting the origin of higher resistivity to be due to a significantly lower (~ 30 times) carrier mobility in the rutile phase.

The nonmetallic behavior of the rutile phase can be attributed to the small Bohr radius of the hydrogen-like donor state in this matrix. According to the Mott transition picture in semiconductors,²¹ the critical donor concentration (n_{dc}) for Mott transition bears the following relation with the Bohr radius (a_H^*) of the hydrogen-like donor state

$$n_{dc} \sim (0.25/a_H^*)^3.$$

Using $a_H^* \sim 2.6$ Å (Ref. 13) of the rutile TiO₂, one can

get the critical concentration n_{dc} of $\sim 10^{21} \text{ cm}^{-3}$. However, the effective donor state Bohr radius for the anatase phase is ~ 15 Å, implying a much lower critical donor density ($5 \times 10^{18} \text{ cm}^{-3}$). Therefore, our rutile phase shows a thermally activated transport behavior while the anatase phase shows a metallic behavior.

In Fig. 4(a), we show the transmittance spectra of the anatase TiO₂ and NTO thin films together with LAO and STO substrates. The evaluated internal transmittance of all films is above 80% in the visible range, suggesting the NTO film grown on LAO is indeed an intrinsic transparent metal. Interestingly, the absorption edge of the film grown on LAO shows a blueshift with niobium doping. It is noticed that the similar result was also reported by Kurita *et al.* very recently.²² This shift may be attributed to the well-known Burstein–Moss effect,²³ usually observed in degenerate semiconductors, where the transition occurs from the filled band to the lowest unfilled level in the conduction band. Based on the assumption of indirect optical transition in anatase TiO₂,¹³

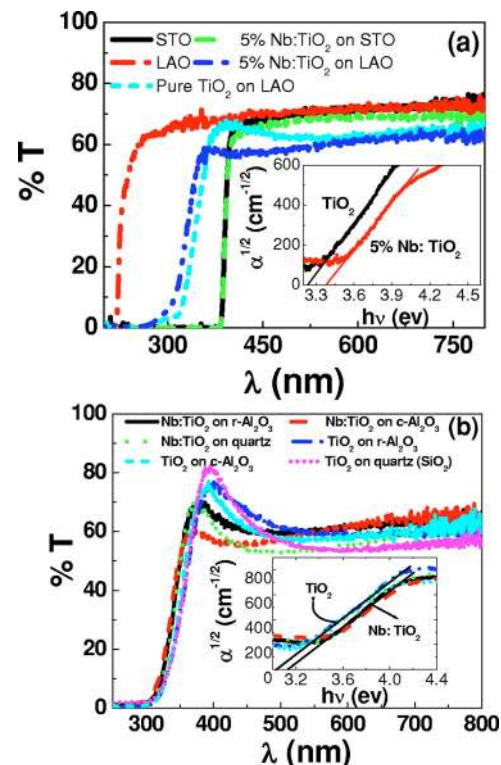


FIG. 4. (Color online) (a) Transmittance spectra of anatase TiO₂, NTO samples and LAO, STO substrates. Inset shows $\alpha^{1/2}$ vs $h\nu$ for TiO₂/LAO and NTO/LAO thin films. (b) Transmittance spectra of rutile TiO₂ and NTO samples. Inset shows $\alpha^{1/2}$ vs $h\nu$.

we plot $\alpha^{1/2}$ as a function of $h\nu$ in the inset of Fig. 4(a), where α is the absorption constant and $h\nu$ is the photon energy. The extrapolated optical absorption edge of TiO₂ and Nb:TiO₂ are found to be 3.22 and 3.37 eV, respectively. If assuming a single parabolic conduction band, one can roughly evaluate the effective mass of the conduction electrons. And our calculation shows this effective mass m^* is $\sim 2.5m_0$, where m_0 is the electron mass. For the sample grown on STO, the absorption edge is dominated by the band edge of the STO substrate itself, forbidding the observation of the expected similar shift in this case.

Figure 4(b) shows the transmittance spectra of the rutile samples with different substrates. We plot $\alpha^{1/2}$ as a function of $h\nu$ in the inset of Fig. 4(b), assuming the indirect optical transition of rutile TiO₂.^{13,24} The extrapolated optical absorption edges of TiO₂ grown on *c*-sapphire, *r*-sapphire, and quartz are ~ 3.09 eV, while those of the NTO films are ~ 3.18 eV. We would like to point out that this shift of rutile NTO films with a magnitude of ~ 0.09 eV is surprising, given the low carrier density (2.5×10^{20} cm⁻³) of these films. If this blueshift is also from the Burstein–Moss effect, calculation based on the simple conduction band assumption will give rise to a very small effective mass $m^* \sim 1.5m_0$, which is unexpected since the effective mass of rutile TiO₂ is usually about $8\text{--}20m_0$,¹³ indicated also by the significantly low Hall mobility in our rutile samples. This large shift may arise from the widening of band gap with niobium doping, as indicated by x-ray photoemission studies.⁶ However, the precise origin of this unusual blueshift requires further investigation.

IV. CONCLUSION

In conclusion, we have grown 5% Nb:TiO₂ films on LAO (001), STO (001), *r*-Al₂O₃, *c*-Al₂O₃, and quartz. Rutherford backscattering channeling data directly reveals the substitution of Nb into a Ti lattice ($\sim 90\%$) for the epitaxial anatase NTO/LAO film, which is found to be an excellent intrinsic conducting oxide ($\rho_{RT} \sim 4.95 \times 10^{-4}$ Ω cm). In contrast, the rutile phase of NTO shows much higher resistivity (2–3 orders higher room temperature resistivity than that of the anatase phase) and a considerably lower mobility. A blueshift in the optical absorption edge is observed in both phases and the magnitude of this shift in rutile is surprisingly large.

ACKNOWLEDGMENTS

The authors would like to thank DARPA (ONR) Program No. N000140210962 for support. They would also like to thank the Center for Superconductivity for student support.

¹D. S. Ginley and C. Bright, MRS Bull. **25**, 15 (2000).

²R. G. Gordon, MRS Bull. **52**, 15 (2000).

³T. Minami, Semicond. Sci. Technol. **20**, S35 (2005).

⁴For review, see F. A. Grant, Rev. Mod. Phys. **31**, 646 (1959); J. B. Goodenough, Prog. Solid State Chem. **5**, 145 (1971); V. E. Henrich, Rep. Prog. Phys. **48**, 1481 (1985).

⁵J. Deford and O. W. Johnson, J. Appl. Phys. **54**, 889 (1983); T. Okamura and H. Okushi, Jpn. J. Appl. Phys., Part 2 **32**, L454 (1993), and references therein; S. A. Chambers, Y. Gao, S. Thevuthasan, Y. Liang, N. R. Shivaparan and R. J. Smith, J. Vac. Sci. Technol. A **14**, 3 (1995).

⁶D. Morris, Y. Dou, J. Rebane, C. E. J. Mitchell, R. G. Egdell, D. S. L. Law, A. Vittadini, and M. Casarin, Phys. Rev. B **61**, 13445 (2000).

⁷S. J. Tauster, S. C. Fung, and R. L. Garten, J. Am. Chem. Soc. **100**, 170 (1978).

⁸D. J. Dwyer, S. D. Cameron, and J. Gland, Surf. Sci. **159**, 430 (1985).

⁹A. Fujishima and K. Honda, Nature (London) **238**, 37 (1972).

¹⁰H. Berger, H. Tang, and F. Lévy, J. Cryst. Growth **130**, 108 (1993).

¹¹N. Hosaka, T. Sekiya, C. Aatoko, and S. Kurita, J. Phys. Soc. Jpn. **66**, 877 (1997).

¹²L. Forro, O. Chauvet, D. Emin, L. Zuppiroli, H. Berger, and F. Lévy, J. Appl. Phys. **75**, 633 (1994).

¹³H. Tang, K. Prasad, R. Sanjinés, P. E. Schmid, and F. Lévy, J. Appl. Phys. **75**, 2042 (1994).

¹⁴H. Tang, F. Lévy, H. Berger, and P. E. Schmid, Phys. Rev. B **52**, 7771 (1995).

¹⁵Y. Matsumoto, M. Murakami, T. Shono, T. Hasegawa, T. Fukumura, M. Kawasaki, P. Ahmet, T. Chikyow, S. Koshihara, and H. Koinuma, Science **291**, 854 (2001).

¹⁶S. R. Shinde, S. B. Ogale, S. D. Sarma, J. R. Simpson, H. D. Drew, S. E. Loafland, C. Lanci, J. P. Biban, N. D. Browning, V. N. Kulkarni, J. Higgins, R. P. Sharma, R. L. Greene, and T. Venkatesan, Phys. Rev. B **67**, 115211 (2003).

¹⁷Y. Furubayashi, T. Hitosugi, Y. Yamamoto, K. Inaba, G. Kinoda, Y. Hirose, T. Shimada, and T. Hasegawa, Appl. Phys. Lett. **86**, 252101 (2005).

¹⁸Q. Wan and T. H. Wang, Appl. Phys. Lett. **88**, 226102 (2006).

¹⁹Y. Furubayashi, T. Hitosugi, and T. Hasegawa, Appl. Phys. Lett. **88**, 226103 (2006).

²⁰S. X. Zhang, S. B. Ogale, L. F. Fu, S. Dhar, D. C. Kundaliya, W. Ramadan, N. D. Browning, and T. Venkatesan, Appl. Phys. Lett. **88**, 012513 (2006); L. F. Fu, N. D. Browning, S. X. Zhang, S. B. Ogale, D. C. Kundaliya, and T. Venkatesan, J. Appl. Phys. **100**, 123910 (2006).

²¹N. F. Mott, Proc. Phys. Soc., London, Sect. A **62**, 416 (1949); N. F. Mott, Philos. Mag. **6**, 287 (1961); N. F. Mott, Adv. Phys. **16**, 49 (1967).

²²D. Kurita, S. Ohta, K. Sugiura, H. Ohta, and K. Koumoto, J. Appl. Phys. **100**, 096105 (2006).

²³E. Burstein, Phys. Rev. **93**, 632 (1954); T. S. Moss, Proc. Phys. Soc. London, Sect. B **67**, 775 (1954).

²⁴J. Pascual, J. Camassel, and M. Mathieu, Phys. Rev. B **18**, 5606 (1978).